HHS Public Access

Author manuscript

*Mol Cancer Ther*. Author manuscript; available in PMC 2019 March 01.

Published in final edited form as:

*Mol Cancer Ther*. 2018 September ; 17(9): 2049–2059. doi:10.1158/1535-7163.MCT-17-1163.

# Role of EphB3 receptor in mediating head and neck tumor growth, cell migration, and response to PI3K inhibitor

**Shilpa Bhatia**[#1], **Anastacia Griego**[#1], **Shelby Lennon**[1], **Ayman Oweida**[1], **Jaspreet Sharma**[1], **Christina Rohmer**[1], **Nomin Uyanga**[1], **Sanjana Bukkapatnam**[1], **Benjamin Van Court**[1], **David Raben**[1], **Christian Young**[2], **Lynn Heasley**[3], and **Sana D. Karam**[1,*]

[1]Department of Radiation Oncology, University of Colorado Denver, Anschutz Medical Campus, Aurora, CO 80045, USA

[2]Department of Pathology, University of Colorado Denver, Anschutz Medical Campus, Aurora, CO 80045, USA

[3]Department of Craniofacial Biology, University of Colorado Anschutz Medical Campus, 12801 E. 17th Ave., MS-8120, Aurora, CO, 80045, USA

[#] These authors contributed equally to this work.

## Abstract

Eph proteins have emerged as critical drivers affecting tumor growth and progression in human malignancies. Our TCGA data analysis showed that EphB3, a receptor tyrosine kinase, is frequently co-amplified with PIK3CA in head and neck squamous cell carcinoma (HNSCC). We therefore hypothesized that EphB3 amplification plays a pro-tumorigenic role in HNSCC and that EphB3 and PIK3CA are co-operating oncogenes that contribute toward its pathogenesis. This hypothesis was not experimentally supported since EphB3 knockdown failed to alter HNSCC tumor cell growth *in vitro* or *in vivo* with an orthotopic model. However, responsiveness of EphB3 knockdown tumors to the PI3K inhibitor, BKM120, was significantly decreased in terms of both tumor growth delay and survival. This is correlated with an increase in pro-survival proteins, S6 and BcL-XL in the EphB3 shRNA tumors treated with BKM120 compared to controls. We further observed that EphB3 knockdown resulted in increased migration *in vitro* and increased EMT gene signature *in vivo.* To explain these results, we examined EphB3 phosphorylation levels in HNSCC at baseline. While total EphB3 levels were high, we found low phospho-EphB3 levels in HNSCCs. Forced EphB3 phosphorylation with an ephrin-B2-Fc fusion protein resulted in decreased HNSCC migration and cell growth and enhanced response to BKM120 *in vitro.* These data collectively indicate that progression of HNSCC selects for low/inhibited EphB3 activity to enhance their survival and migratory abilities and decrease response to PI3K signaling. Therefore, strategies focused on activating EphB3 might be helpful to inhibit tumor growth and enhance sensitivity to PI3K inhibitors in HNSCC.

[*]**Corresponding author:** Sana D. Karam, MD, Ph.D., Mailing address: Department of Radiation Oncology, 1665 Aurora Court Suite 1032, Aurora, CO-80045, Phone: 720-848-0910, Fax: 720-848-0238, sana.karam@ucdenver.edu.

Conflict of interest

The authors have no conflict of interest.

**Keywords**

EphB3; migration; head and neck cancer; PI3K inhibitor

## Introduction

Scientific developments over the past few years have enhanced our understanding of dysregulated cell signaling pathways potentiating cancer progression, and Eph receptors have emerged as attractive candidates for therapeutic intervention. The paradoxical nature of Eph activities in different cancer types (1), however, poses a significant challenge, and we are now beginning to understand the dichotomy of Eph receptors and how their dysregulated expression can promote or inhibit tumor progression.

EphB3 is a receptor protein tyrosine kinase that interacts with ephrin-B ligands to trigger downstream signaling and has been reported as a key player in multiple cancers (2–5). For instance, EphB3 has been shown to play a tumor-suppressor function in colorectal cancer (4–7). In non-small cell lung cancer (NSCLC), disparate functions for EphB3 have been described (2,3). A report by Ji *et al.*, has described significant upregulation of EphB3 in both patient tumor specimens and cancer cell lines and a correlation was observed between EphB3 levels and patient pathological features (3). They further documented that high levels of EphB3 increased proliferation and migration both *in vitro* and *in vivo* in a kinase-independent manner (3). Furthermore, knockdown of EphB3 resulted in decreased tumorigenesis and metastasis *in vivo (3)*. A study published by the same research group showed that EphB3 receptor is hypophosphorylated in 75% of NSCLC samples, despite its high expression levels (2). Forced activation of EphB3 kinase in EphB3-overexpressing NSCLC cancer cells was shown to inhibit cell migratory capability *in vitro* as well as in metastatic seeding *in vivo* (2).

Interrogation of the TCGA database led us to identify EphB3 as a new gene target with high copy number amplification in head and neck squamous cell carcinoma (HNSCC). Further, we found that both EphB3 and PI3KCA, present on chromosome 3q (8), are frequently co-amplified in HNSCC. We therefore hypothesized that EphB3 amplification plays a pro-tumorigenic role in HNSCC and that EphB3 and PIK3CA are co-operating oncogenes that contribute toward its pathogenesis. We undertook a loss of function approach with shRNA knockdown to examine the effects on HNSCC growth, migration, and sensitivity to PI3K inhibitors. Our data surprisingly showed that EphB3 knockdown does not alter tumor growth, but promotes migration, upregulation of epithelial-to-mesenchymal transition (EMT) and decreases responsiveness to PI3K inhibitors. In light of these data, which refute our original hypothesis, we subsequently found that despite high levels of total EphB3, low levels of baseline EphB3 phosphorylation are observed in HNSCC. Furthermore, forced phosphorylation of EphB3 with ephrin-B2-Fc fusion protein decreased HNSCC migration and cell growth, and enhanced responsiveness of these cells to PI3K inhibitor. These novel findings improve our understanding of the role of EphB3 in HNSCC and provide a potential therapeutic strategy for the treatment of this cancer, particularly in the setting of PI3K inhibitors.

## Materials and methods

### TCGA Data Analysis

Whole Genome Sequences from all cancer type cohorts (27 cohorts total) of The Cancer Genome Atlas (TCGA) (http://cancergenome.nih.gov) were accessed via cBioPortal (http://cbioportal.org) and queried for any genomic alterations in EPHB3. Cohorts containing significant amplification of EPHB3 including Head and Neck Provisional (n=530), Lung Squamous Cell Carcinoma Provisional (n=530), and Cervical Cancer Provisional (n=309) were re-queried for alterations in PIK3CA gene commonly found altered in head and neck cancers. EPHB3 is mentioned in RSEM (RNA-Seq by Expectation Maximization) units.

For survival analysis, the HNSCC RNAseq dataset was downloaded from the cancer genome atlas (TCGA) and patients with oral cavity tumors (n=314) were selected. For the purpose of this study, classifications of alveolar ridge, buccal mucosa, lip, oral tongue, and floor of mouth were re-classified to oral cavity. Patients were sorted by EPHB3 gene-expression and divided into quartiles. Patients in the upper quartile were classified as high EPHB3 and patients in the lower quartile were classified as low EPHB3. Overall survival and disease-free survival was calculated by Kaplan–Meier method using log-rank tests for comparisons. Univariate Cox proportional model was used to calculate the Hazard ratio (HR). Two-sided P-values were reported for all survival analyses.

### Cell lines and reagents

The human HNSCC cell lines CAL27 and Fadu were obtained from the American Type Culture Collection (ATCC, Rockville, MD, USA). MSK921, and Detroit 562 cell lines were obtained from Dr. XJ Wang's lab (University of Colorado, Anschutz Medical Campus, Aurora, CO, USA). MSK921 cells were maintained in RPMI-1640 medium (Gibco). CAL27, Fadu, UM-SCC25, UM-SCC1, and Detroit 562 cells were maintained in Dulbecco's Modified Eagle's Medium (DMEM) (Gibco). All these cell lines were authenticated by STR testing. Murine B4B8 and LY2 squamous cell carcinoma cells were obtained from the lab of Dr. Nadarajah Vigneswaran (UTHealth, Houston, TX). Both these cell lines were maintained in DMEM/F12 (Gibco). MOC1, MOC2 cell lines were obtained from the lab of Dr. Young J. Kim (Johns Hopkins University, Baltimore, MD) whereas MEER and MOE cell lines were obtained from Dr. John Lee (Sanford Health, Sioux Falls, SD). All cell lines were grown in the presence of 10% fetal bovine serum (FBS) and primocin at 37°C, 5% $CO_2$ and checked for mycoplasma contamination. The class I PI3K inhibitor, BKM120, was purchased from Selleck Bio chemicals (Houston, TX, USA) and prepared as 100 mM stocks in DMSO with aliquots stored at −20ºC.

### Generation of shRNA knockdown clones

Lentivirus encapsidated shRNA vectors (Sigma, pLKO.1) were purchased from the University of Colorado Cancer Center Functional Genomics Facility (Anschutz Medical Campus, Aurora, CO). EphB3 knockdown was achieved by transducing cells with shRNA against human EphB3 (Sigma-Aldrich catalog # TRCN0000006428) or mouse EphB3 (Sigma-Aldrich catalog # TRCN0000023351). Cells were transduced with control shRNA (Sigma-Aldrich catalog # SHC016) in parallel. Transduced cells were selected with 1 μM or

6 μM (CAL27 and Ly2, respectively) puromycin and following selection, cells were maintained in 1 μM dose. For Cal27 cell lines, we were able to generate four viable clones with EphB3 knockdown. For Ly2 cell line, A and B were the viable clones we were successfully able to generate and expand for experiments. We used the clones that showed ~ 60% knockdown compared to control shRNA group.

### Viability assay

CAL27 cells (Control shRNA and EphB3 knockdown clones) were seeded at a density of 150,000 cells per well in six-well plates and maintained in complete growth medium containing 10% FBS and primocin. Approximately 72 h post-plating, cells were fixed with 10% TCA (LabChem, Zelienople, PA, USA) and viability was measured by sulforhodamine B (SRB) assay (ACROS Organics). For trypan blue assay, cells were collected by trypsinization. To each 10 μL aliquot of cells, 10 μL of trypan blue dye was added. Cell counting was performed using an automated T-20 cell counter (Bio-Rad, Hercules, CA, USA). The experiment was replicated twice and each condition had 3–4 replicates.

### Stimulation with clustered-Fc protein

Control ChromoPure mouse IgG-Fc fragment (Jackson ImmunoResearch Laboratories) or rmEphrinB2-Fc chimera (R&D Systems, Minneapolis, MN, USA) was pre-clustered with anti-hIgG1 Fc antibody (R&D Systems) at a 1:3 ratio for 30 minutes at 4$^{o}$C with shaking. Pre-clustering ensures rapid and effective receptor activation once ligands come into contact range. Pre-clustered Fc protein was added to cell culture media at a final concentration of 3 μg/mL. Cells were stimulated with pre-clustered ligand for 15 minutes at 37$^{o}$C. Following stimulation, cells were transferred to ice and washed two times with 1X cold PBS. Cells were detached by scraping and transferred to a microfuge tube. Cells were pelleted, supernatant removed, and pellet was lysed in 1X cold Cell Lysis Buffer (Cell Signaling, Danvers, MA, USA) containing 1x Halt Protease Inhibitor Cocktail (Thermo Scientific, IL, USA) and Phosphatase Inhibitor Cocktail 2 (Sigma, MO, USA). Protein concentration was determined by BCA assay (Thermo Scientific).

### Immunoprecipitation

Frozen tumors were pulverized in liquid nitrogen using a mortar and pestle followed by resuspension in 1X Cell Lysis Buffer containing protease and phosphatase inhibitors. Lysate was diluted to 2 μg/μl in lysis buffer and 250 μl of resulting lysate was incubated with 1:100 dilution of anti-EphB3 antibody (Sigma) overnight at 4$^{o}$C with end-over-end rotation. Magnetic protein G beads (BioRad, Hercules, CA, USA) were washed three times with 1X PBS prior to adding lysate-antibody complexes. Beads were incubated with lysate-antibody complexes for 1 h at 4$^{o}$C with end-over-end rotation. Beads were washed three times with cold 1:1 lysis buffer:PBS, removing supernatant after each wash. Protein was eluted from beads by adding 1x Sample Loading Buffer (Invitrogen) containing 1X sample reducing agent (Invitrogen) and boiling beads at 95$^{o}$C for 15 min. 200 μg equivalent starting material was resolved on a 10% SDS-PAGE gel and transferred to Immuno-Blot PVDF membrane (BioRad). Membranes were probed for total phospho-tyrosine (Cell Signaling) prior to stripping (Restore PLUS Western Blot Stripping Buffer, Thermo Scientific) and reprobed for

total EphB3 protein (Abcam, Cambridge, MA, USA). The immunoprecipitation assay was repeated twice.

### Boyden Chamber Migration Assay

CAL27 cells or LY2 were serum starved overnight prior to seeding ($2.5\times 10^5$ cells/well) in serum-free media into the upper chamber of a 24 well plate insert with 8.0 μM pores (BioCoat Control Inserts, BD). Bottom chamber was filled with appropriate media containing 10% FBS and pre-clustered control-Fc or ephrinB2-Fc (R&D Systems). Cells were incubated in a 37°C cell culture incubator and allowed to migrate for 48 h (CAL27) or 24 h (LY2). To prepare membranes for imaging, un-migrated cells in the upper chamber were removed according to manufacturer's instructions and migrated cells were stained in 0.1% crystal violet (10% methanol), washed in $dH_2O$, and allowed to dry overnight before membrane was cut and mounted on a microscope slide with immersion oil. An image of the membrane was taken at 4x magnification and number of migrated cells was counted using ImageJ software (NIH). Experiment was repeated 2–3 times. Each condition had three replicates.

### Generation of CAL27 BKM120 resistant cell line

CAL27 cells were continually cultured in increasing doses of BKM120 (1.5, 2.0, and 2.5 μM) until the cells were able to survive and proliferate in 2.5 μM BKM120. Parental and BKM120-resistant CAL27 cells were plated in drug-free media overnight. The following day the cells were treated with DMSO or 2.5 μM BKM120. After 72 h incubation, relative cell abundance was assessed by SRB assay.

### Cell growth assay

CAL27 cells were seeded at a density of 2000 cells/well in a 96-well plate and stimulated with pre-clustered Control-Fc or ephrin-B2-Fc as described earlier. Cells were stimulated again at 48 h, and 72 h post-plating. Changes in cell growth between stimulated and non-stimulated groups were analyzed by MTT assay by reading the absorbance at 595 nm on a microplate reader. Data was plotted as % cell growth normalized to 24 h time-point from multiple replicates per experimental condition.

### Western blotting

HNSCC cells transfected with control or EphB3 shRNA and tumor tissues treated with vehicle or BKM120 inhibitor treatment were harvested. Cells or tumor tissues were homogenized in RIPA lysis buffer (Millipore, Billerica, MA, USA), containing protease inhibitor cocktail (Thermo Fisher Scientific Inc., IL, USA) and phosphatase inhibitor (Sigma, MO, USA) on ice for 30 min. The homogenate was centrifuged at 4°C at 13,000 rpm for 20 min, and lysates were collected. Protein concentration was determined using the BCA Protein Assay kit (Thermo Fisher Scientific Inc., IL, USA). Lysates (20–30 μg) were loaded onto 10–12% SDS-PAGE gels. Electrophoresis, blocking, probing, and detection of proteins were conducted as described earlier (9). Membranes were probed overnight at 4°C with respective antibodies. All primary antibodies against p-AKT (S473), AKT, p-S6 (S235/S236), S6, Bcl-XL were obtained from Cell Signaling Technology (Danvers, MA, USA).

Anti-EphB3 antibody was obtained from Sigma (St. Louis, MO, USA). Horseradish peroxidase (HRP)–conjugated secondary antibodies were obtained from Sigma (St. Louis, MO, USA). The experiment was replicated two times.

### *In vivo* studies

Female athymic nude mice (6 weeks old, n=13–15) were purchased from Envigo (Indianapolis, In, USA). All mice were handled in accordance with the ethics guidelines and conditions set and overseen by the University of Colorado, Anschutz Medical Campus Animal Care and Use Committee. All protocols for animal studies were reviewed and approved by the Institutional Animal Care and Use committee at the University of Colorado, Anschutz Medical Campus. CAL27 shRNA control and EphB3 shRNA transduced cells were injected into the right buccal cavity at $1\times10^6$ cells/mouse in 1:1 serum-free media:matrigel ratio. BKM120 was administered at a dose of 30 mg/kg daily by oral gavage for a total duration of two weeks (five days/week) in 1:9 1-methyl-2-pyrrolidone:PEG300 for a total of 10 doses of drug. A mix of 1-methyl-2-pyrrolidone:PEG300 solution (1:9 ratio) was used as a vehicle. Tumor growth was measured twice a week using a digital caliper and tumor volume was calculated using the formula: $[(\text{smaller diameter})^2 \times (\text{longer diameter})]/2$. Tumors harvested between days 25–45 post-implantation were used for western blotting and immunohistochemical analysis. Survival analysis was performed using Kaplan-Meir survival curves. For *in vivo* studies, survival was calculated based on animal death dictated by tumor volume guidelines (maximum limit: 2000 $mm^3$) approved in our animal protocol and loss of 20% of total body weight.

### Immunohistochemistry

Immunohistochemical analysis was performed using an established protocol (10) on tumors harvested from mice implanted with either CAL27 Control shRNA or CAL27 EphB3 knockdown clones treated with Vehicle or BKM120 using anti-PCNA antibody (1:100 dilution, BD biosciences, San Jose, CA, USA), E-Cadherin, and Vimentin (1:100 dilution, Cell Signaling). This was followed by incubation with biotinylated goat anti-mouse IgG or biotinylated goat anti-Rabbit IgG secondary antibody (1:400 dilution, Vector Laboratories, Burlingame, CA, USA). Images were captured using a 20x objective on a Nikon microscope. At least 4–5 images were captured per tumor section. The quantification was performed by counting the no. of positive cells or positive area per high power field using Image J software.

### Statistical analysis

All the experiments were performed in duplicate or triplicate and repeated two to three times. Quantitative analyses were performed using Student’s t test or one-way ANOVA by GraphPad Prism software. A p-value of $<0.05$ was considered significant.

## Results

### EphB3 is amplified in head and neck cancer

Alterations in EPHB3 across cancer types in the TCGA database were accessed via cBioportal and analyzed. We found that EPHB3 is amplified in multiple human carcinomas,

including head and neck squamous cell cancer (HNSCC) (Figure 1A). We also performed analysis of microarray gene-expression in 30 head and neck cancer cell lines from the Cancer Cell Line Encyclopedia. We found, similar to patients, a wide range of EPHB3 expression (Supplementary Figure 1). To confirm these data, we examined EphB3 protein levels in multiple human (Figure 1B) and murine head and neck cancer cell lines (Figure 1C). Total EphB3 protein levels was found to be variable in multiple human and murine HNSCC, compared to normal respective negative control tissue of adult cerebellum (11) and NIH 3T3 cells (Figures 1B, 1C). We also observed some variation in EphB3 levels in human HNSCC cell lines when compared with normal oral keratinocyte (NOK) cell line (Supplementary Figure 2A, 2B).

### Knockdown of EphB3 does not affect cell viability *in vitro* but increases cell migration

To elucidate the role of EphB3 receptor in HNSCCs, we knocked down the levels of the receptor in both human and murine head and neck cancer cell lines using EphB3-targeting shRNA. Compared to the control transfectants, CAL27 and Ly2 cells transfected with EphB3-specific shRNA showed approximately 55–80% reduction in the EphB3 levels (Figures 2A and2B). Our data demonstrated that reduced EphB3 expression in CAL27 cells (Figure 2C) or Ly2 cells (Supplementary figure 3A) did not significantly alter tumor cell viability when compared to the control shRNA group. These data were substantiated by SRB assay (Figure 2D). EphB3 receptor has previously been reported to play a role in tumor cell migration in non-small cell lung cancer (2). Therefore, we investigated whether shRNA-mediated knockdown of EphB3 would affect cell migration in HNSCC cells using a Boyden chamber assay. A significant increase in migration was evident in EphB3-knockdown CAL27 cells compared to the cells that were transfected with control shRNA (Figure 2E). In Ly2 cells, cells were EphB3 was knocked down also showed a trend towards increased migration compared to the control counterpart (Supplementary figure 3B).

### EphB3 and PIK3CA are frequently co-amplified in squamous cell carcinomas including HNSCC

Given that PI3K activity has been shown to modulate Eph/ephrin proteins (12,13) we sought to establish if there is any correlation between EphB3 and PI3KCA as both genes being located on chromosome 3. Genomic alterations in the TCGA database were analyzed for head and neck cancer (n=530), lung squamous cell carcinoma (n=530), and cervical squamous cell carcinoma and endocervical adenocarcinoma (n=309) (Figure 3A). It was noted that ~18–43% patients have co-amplification of EPHB3 and PIK3CA, a catalytic subunit of PI3K (Figure 3A, Table 1). We also analyzed the levels of PI3 Kinase p110α subunit in our panel of human HNSCC cells and observed variable expression (Supplementary figure 2A, 2C).

### EphB3 downregulation decreases sensitivity to PI3K inhibitor *in vitro* in head and neck cancer cells

To determine the role of EphB3 in PI3K signaling inhibition, we generated PI3K inhibitor resistant CAL27 cell line. CAL27 cells were grown in the presence of increasing concentrations of BKM120, a pan-class I PI3K inhibitor (14), until they had acquired resistance to 2.5 μM BKM120. SRB proliferation assay demonstrates that CAL27-BKM120-

resistant cells proliferate more slowly than parental CAL27 cells but are less sensitive to BKM120 treatment than parental cells which are acutely sensitive to BKM120 (Figure 3B). DMSO at the same concentration as BKM120 was used as a negative control. Further, we exposed CAL27 parental and BKM120 resistant cells to increasing doses of BKM120. Western blot data demonstrates that exposure of parental CAL27 to PI3K inhibitor for 24 h decreased the level of EphB3 while the BKM120-resistant cells maintained constitutively low levels of EphB3 (Figure 3C). Parental CAL27 cells treated with BKM120 had reduced levels of p-AKT and p-S6, downstream effectors of PI3K signaling pathway (Figure 3C). Levels of p-AKT and p-S6 were increased in CAL27 BKM120-resistant cell line following short-term withdrawal of the BKM120 (Figure 3C). The p-AKT and p-S6 levels were subsequently reduced after exposure to the PI3K inhibitor for 24 h, (Figure 3C). The densitometric analysis for this panel is presented in Table 2. In addition, we analyzed these markers in CAL27 cell line stably expressing control or EphB3-specific shRNA treated with vehicle or BKM120. The data show a minor increase in the levels of p-AKT and p-S6 in the CAL27 EphB3 knockdown clones compared to the control shRNA cells in the absence of BKM120 inhibitor. The levels of p-S6 protein are slightly increased in the EphB3 knockdown cells compared to the control samples in the presence of high dose of BKM120 (Figure 3D). The densitometric analysis is presented in Table 3. These data demonstrate an association between decreased sensitivity to PI3K inhibition and decreased EphB3 levels.

## EphB3 knockdown does not significantly alter tumor growth and survival but decreases sensitivity to PI3K inhibitor in an orthotopic model of head and neck cancer

Based on the *in vitro* findings and TCGA data, we next evaluated the effect of EphB3 knockdown on tumor growth *in vivo* using CAL27 cell line stably expressing control shRNA or EphB3 shRNA. Because the complex interplay between Eph receptors and ligands is highly context specific, it is best modeled *in vivo*. To closely mimic the tumor microenvironment, tumor cells were implanted orthotopically in the buccal region of nude mice. Orthotopic tumors best recapitulate characteristics of an aggressive tumor growth model to study genetic and molecular changes associated with tumor progression and development (15). They also serve as useful tools to study the efficacy of therapeutic agents (15). In our experimental model, we observed that knockdown of EphB3 did not significantly affect CAL27 tumor growth compared to the control group (Figure 4A). Due to the aggressive tumor growth pattern, most of the mice in the EphB3 knockdown and control group subjected to vehicle treatment were sacrificed after day 20 post-vehicle treatment.

We also interrogated whether EphB3 knockdown in head and neck cancer cells alters *in vivo* sensitivity towards PI3K inhibition. We found that EphB3 knockdown in CAL27 tumors that were administered with BKM120 had significantly enhanced tumor growth by approximately1.5 fold compared to the control BKM120 treated xenografts at day 42 post-treatment with BKM120 (Figure 4B).

In addition, we investigated whether EphB3 knockdown in CAL27 tumors had an effect on overall survival *in vivo*. Kaplan Meier survival curves show that mice implanted with CAL27 knockdown tumors had a median survival of 25 days compared to mice implanted with CAL27 control tumors where the median survival was approximately 38 days (Figure

4C). Treatment of CAL27 control tumors with BKM120 also provided survival benefit compared to other groups with median survival of approximately 70 days (Figure 4C). However, EphB3 knockdown tumors treated with BKM120 reduced the median survival to 50 days (Figure 4C).

To determine proof-of-target, we performed an immunoprecipitation assay to detect the phosphorylation status of EphB3 in the control vehicle vs. EphB3 knockdown tumors treated with vehicle or BKM120. We observed decreased levels of p-EphB3 in CAL27 EphB3 knockdown tumor xenografts (Figure 4D). Further comparisons between the BKM120 treated groups show reduction in the p-EphB3 levels following EphB3 receptor downregulation compared to the control BKM120 treatment (Figure 4D). We also analyzed the levels of the pro-survival proteins, p-S6, S6, p-AKT, AKT, and Bcl-XL, in the tumors harvested from control and EphB3 knockdown groups treated with vehicle or BKM120 treatment. Our data show a decrease in the pro-survival protein levels of p-S6, S6, AKT, and Bcl-XL in control tumors treated with BKM120 (Figure 4E). An increase in the levels of p-S6, p-AKT were observed in EphB3 shRNA knockdown tumors following BKM120 treatment compared to similarly treated control transfectants (Figure 4E).

## EphB3 knockdown decreases sensitivity towards BKM120 treatment by affecting markers of tumor cell proliferation and migration *in vivo*

Given that our *in vitro* data showed an increase in HNSCC migration following EphB3 knockdown, we sought to determine the mechanisms underlying changes in tumor cell growth observed *in vivo* particularly following BKM120 inhibitor treatment. Immunohistochemical analysis on tumor sections was performed on tumors derived from EphB3 knockdown and control tumors with vehicle or BKM120 treatment. Our data show that knockdown of EphB3 did not affect tumor cell proliferation to a significant extent compared to the control vehicle as evident by PCNA staining (Figure 4F). The CAL27 tumors treated with BKM120 showed reduced PCNA staining compared to the control vehicle treated group (Figure 4F). However, when tumors with EphB3 knockdown were treated with BKM120, a significant increase in the levels of PCNA was observed compared to control BKM120 and EphB3 KD vehicle (Figure 4F), suggesting that EphB3 knockdown decreases response to BKM120 inhibitor treatment and results in increased tumor cell proliferation.

Since we observed an increase in migration of EphB3 knockdown cells *in vitro*, we also analyzed the levels of E-cadherin (an epithelial cell marker) and vimentin (a mesenchymal marker), proteins reported to play a role in tumor cell migration (16,17). These two proteins with opposing roles have long been considered as key components of epithelial-mesenchymal-transition (EMT) in various cancers (16,17). The cells that undergo the process of EMT are characterized by morphological transformation, alteration in the levels of EMT markers that in turn affects cell motility (16,17). Downregulation of E-cadherin function or expression and gain of function or elevated levels of vimentin has been reported to play a role in cancer progression and metastasis (18,19). We observed significant upregulation of E-cadherin in control tumors treated with BKM120 compared to the non-treated counterparts (Figure 4G). However, when EphB3-deficient tumors treated with

BKM120 inhibitor were analyzed, we observed significant reduction in E-cadherin expression compared to the control tumors that were subjected to the same treatment (Figure 4G). Vimentin is an EMT marker that plays a critical role in tumor cell migration and metastasis. Consistent with an EMT phenotype, immunohistochemical analysis showed that EphB3 downregulation significantly enhanced the levels of vimentin compared to the control tumors treated with vehicle (Figure 4H). However, when the control tumors were treated with PI3K inhibitor, there was a significant reduction in vimentin expression compared to control vehicle group (Figure 4H).

## EphB3 is present in an inactive state and forced phosphorylation with ephrin-B2-Fc stimulation decreases migration, cell growth, and enhances responsiveness to BKM120 *in vitro*

Our data suggest that HNSCC selects for low or inhibited EphB3 activity to enhance their survival and migratory abilities and decrease response to PI3K signaling. To reconcile the unexpected data, which refutes the original hypothesis that EphB3 amplification by HNSCC is indicative of pro-tumorigenic role and rather supportive of a hypothesis that EphB3 exerts a suppressor role, we assessed the activation of EphB3 by examining its phosphorylation status at baseline. We found that although the basal level of EphB3 was detectable in both CAL27 and Ly2 cells, the basal phospho-EphB3 levels were low (Figure 5A and5B). Stimulation with ephrin-B2 Fc increased the levels of phosphorylated form of EphB3 (Figure 5A and5B). Additionally, forced phosphorylation with ephrin-B2-Fc stimulation significantly decreased CAL27 HNSCC migration in a Boyden chamber assay (Figure 5C) and cell growth by MTT assay (Figure 5D) Furthermore, we observed a significant reduction in cell growth when ephrin-B2 stimulated CAL27 cells were treated with BKM120 compared to the Control-Fc treated group (Figure 5E).

To further understand why HNSCC cell lines amplify EphB3 RNA levels while simultaneously inactivating it, we examined the levels of its ligand ephrin-B2. Ephrin-B2 is membrane bound that signals via reverse signaling and this has been shown to play a critical role in promoting pro-tumorigenic roles in different cancer subtypes (20,21). Furthermore, we have established it to be a negative prognostic factor in HNSCC (22). Evaluation of Western blot analysis shows variable levels of ephrin-B2 protein in human and mouse HNSCC cell lines (Figure 5F, 5G). Analysis of the phosphorylation status of EphB3 in CAL27 and Ly2 cells transfected with control shRNA and EphB3-specific shRNA by immunoprecipitation analysis shows reduced levels of p-EphB3 present in both CAL27 (Figure 5H) and Ly2 cells (Figure 5I) transfected with EphB3-specific shRNA as compared to the control shRNA clones.

## High EphB3 expression correlates with better overall and disease-free survival in HNSCC patients

Given that our findings support a model where activation of EphB3 acts in a suppressive role in HNSCC, we interrogated survival outcomes in the TCGA RNAseq dataset. Patients with oral cavity tumors (n=314) were sorted by EphB3 gene expression and divided into quartiles (Figure 6A). Patients in the upper quartile (Q1) were classified as high EphB3 cohort and those with lower quartile (Q4) were classified as low EphB3 cohort (Figure 6A). Survival

analysis revealed a trend that patients with high EphB3 expression have better overall survival (median overall survival ~ 49 months) compared to the patients with low EphB3 expression (median overall survival ~ 28 months) (Figure 6B). Patients with high EphB3 expression also showed significantly higher disease-free survival rates with median survival ~71 months as compared to the patients with low EphB3 expression with median survival ~28 months (Figure 6C).

## Discussion

The family of Eph receptor tyrosine kinases has garnered attention of the scientific community due to their role in both physiologic and pathologic processes (23–25). Dysregulated expression of both Eph receptors and their cognate ligands has been reported to contribute towards tumor progression, and metastasis (23). Aberrant expression of EphB3, a member of the Eph receptor gene family, has been reported in different cancers (2–4). In colorectal cancer, a tumor suppressor function has been described for EphB3 where its loss has been shown to result in invasive cancer in the Apc (min/+) mice (5) and acts as an inhibitor of tumor cell metastasis by regulating intercellular adhesive and repulsive interactions (5). In NSCLC, EphB3 has been found to be amplified, but its silencing suppressed tumor growth and metastasis (3). Yet, in a different manuscript done by the same group a year later, it was reported that inhibition of EphB3 promoted NSCLC migration and metastasis (2). This perplexing dichotomy was attributed to differences in kinase activation status of the EphB3 receptor, whereby it acts as a tumor promoter via “kinase independent” properties and as a tumor suppressor via “kinase dependent” properties.

To our knowledge this is the first study that investigates EphB3 expression and function in HNSCC. We found that EphB3 is overexpressed in the TCGA HNSCC dataset and is co-amplified with PI3KCA. Given that the high levels of expression and the association between Eph receptor tumor promoting properties and the AKT pathway (2,12), we hypothesized that EphB3 amplification plays a pro-tumorigenic role in HNSCC and that EphB3 and PIK3CA are co-operating oncogenes that contribute toward its pathogenesis. Our results unexpectedly showed that the EphB3 shRNA knockdown approach had no significant effect on cancer cell viability *in vitro* as determined by trypan blue staining and SRB assay, but it increased HNSCC migration, increased EMT markers, and reduced sensitivity to PI3K inhibitors. Furthermore, we found that high EphB3 RNA expression levels correlate with improved disease-free survival outcomes. This led us to investigate the activation or phosphorylation status of the protein at baseline in this context. Our data show that EphB3 is hypo-phosphorylated at baseline and forced phosphorylation with ephrin-B2 stimulation decreases migration, cell growth, and enhances response to PI3K inhibitor. These results are consistent with the published literature showing that EphB3 receptor activation decreases invasion, migration, and metastasis in NSCLC (2), colorectal cancer (5), and hepatoblast migration (26). Knockdown of EphB3 also reduced sensitivity to BKM120 via an increase in AKT and p-S6 proteins. The altered effects on tumor growth and sensitivity to PI3K inhibitor observed in our tumor model were associated with changes in the expression level of proteins known to play a role in the cell proliferation, survival, and cell migration. PI3K–AKT–mTOR pathway alterations are implicated in almost a third of HNSCC, with PIK3CA commonly mutated and multiple PI3K–AKT–mTOR pathway aberrations associated with

disease progression (27,28). In the recent article published by Swick et al., combined inhibition of PI3K/AKT/mTORC and RAS/RAF/MAPK1 signaling resulted in significant tumor growth inhibition (28). However, the clinical success of agents targeting these pathways have shown limited success. Therefore, it justifies the need to look for alternate agents that can be exploited to maximize the therapeutic response. Our data suggests that EphB3 knockdown reduces sensitivity to PI3K inhibitors. Therefore, a novel generation of compounds that can enhance the activated levels of EphB3 in tumors might show some promise in combination with PI3K inhibitors.

To explain the biology of why a tumor suppressor gene would be amplified, we examined the status of its cognate ligand, ephrin-B2. The biology of EphB-ephrinB signaling is highly complex because both the receptor and ligand can signal upon cell to cell contact (23). Forward signaling from the EphB receptor requires the ectodomain of ephrin-B2 for activation whereas reverse signaling from ephrin-B2 ligand requires the ectodomain of an EphB receptor to signal. Signaling mediated by either a receptor or a ligand or both (bidirectional) can be activated during cell-to-cell interaction and leads to an effect. Activation of ephrin-B2 signaling has been shown to trigger tumorigenesis, a process mediated in part by a pro-angiogenic effect (20,21,29). Our published analysis showed that ephrin-B2 acts as a prognostic indicator of overall survival and response to both chemotherapy and RT in patients with high-risk HNSCCs (22). We also showed that inhibition of ephrin-B2 signaling results in tumor growth retardation in patient derived xenograft models of high risk HNSCC (22). In the current study, we show elevated levels of ephrin-B2 in various HNSCCs cell lines. This suggests that cancer cells selects for low or inhibited tumor suppressor activity while at the same time using its ectodomain to stimulate the oncogenic effect of a tumor promoter. However, given the redundancy of EphB receptor expression in HNSCC, with EphB4 being another ephrin-B2 binding receptor that is ubiquitously expressed, the effect of targeted deletion of EphB3 on ephrin-B2 activation and cell proliferation can potentially be compensated.

In conclusion, our study provides the first evidence establishing the role of EphB3 in head and neck cancers and modulated response to PI3K signaling inhibition. Future studies are warranted to understand the underlying mechanism and interaction between EphB3 receptor and PIK3CA signaling component in our model system that in turn will guide the development of novel therapeutic agents applicable for head and neck cancer patients.

## Supplementary Material

Refer to Web version on PubMed Central for supplementary material.

## Acknowledgements

This work was supported by the funding awarded to S.D. Karam by the National Institutes of Health under Ruth L. Kirschstein National Research Service Award (T32CA17468), Paul Calabresi Career Development Award for Clinical Oncology (K12) CA086913, and the RSNA grant (RSD1713).

Financial Information

This work was supported by the funding awarded to S.D. Karam by the National Institutes of Health under Ruth L. Kirschstein National Research Service Award (T32CA17468), Paul Calabresi Career Development Award for Clinical Oncology (K12) CA086913, and the RSNA grant (RSD1713).

## References

1. Noren NK, Pasquale EB. Paradoxes of the EphB4 receptor in cancer. Cancer Res 2007;67(9):3994–7 doi 10.1158/0008-5472.CAN-07-0525. [PubMed: 17483308]
2. Li G, Ji XD, Gao H, Zhao JS, Xu JF, Sun ZJ, et al. EphB3 suppresses non-small-cell lung cancer metastasis via a PP2A/RACK1/Akt signalling complex. Nat Commun 2012;3:667 doi 10.1038/ncomms1675. [PubMed: 22314363]
3. Ji XD, Li G, Feng YX, Zhao JS, Li JJ, Sun ZJ, et al. EphB3 is overexpressed in non-small-cell lung cancer and promotes tumor metastasis by enhancing cell survival and migration. Cancer Res 2011;71(3):1156–66 doi 10.1158/0008-5472.CAN-10-0717. [PubMed: 21266352]
4. Chiu ST, Chang KJ, Ting CH, Shen HC, Li H, Hsieh FJ. Over-expression of EphB3 enhances cell-cell contacts and suppresses tumor growth in HT-29 human colon cancer cells. Carcinogenesis 2009;30(9):1475–86 doi 10.1093/carcin/bgp133. [PubMed: 19483190]
5. Batlle E, Bacani J, Begthel H, Jonkheer S, Gregorieff A, van de Born M, et al. EphB receptor activity suppresses colorectal cancer progression. Nature 2005;435(7045):1126–30 doi 10.1038/nature03626. [PubMed: 15973414]
6. Ronsch K, Jagle S, Rose K, Seidl M, Baumgartner F, Freihen V, et al. SNAIL1 combines competitive displacement of ASCL2 and epigenetic mechanisms to rapidly silence the EPHB3 tumor suppressor in colorectal cancer. Mol Oncol 2015;9(2):335–54 doi 10.1016/j.molonc.2014.08.016. [PubMed: 25277775]
7. Jagle S, Ronsch K, Timme S, Andrlova H, Bertrand M, Jager M, et al. Silencing of the EPHB3 tumor-suppressor gene in human colorectal cancer through decommissioning of a transcriptional enhancer. Proc Natl Acad Sci U S A 2014;111(13):4886–91 doi 10.1073/pnas.1314523111. [PubMed: 24707046]
8. Isaacsson Velho PH, Castro G, Jr., Chung CH Targeting the PI3K Pathway in Head and Neck Squamous Cell Carcinoma. Am Soc Clin Oncol Educ Book 2015:123–8 doi 10.14694/EdBook_AM.2015.35.123.
9. Bhatia S, Baig NA, Timofeeva O, Pasquale EB, Hirsch K, MacDonald TJ, et al. Knockdown of EphB1 receptor decreases medulloblastoma cell growth and migration and increases cellular radiosensitization. Oncotarget 2015;6(11):8929–46 doi 10.18632/oncotarget.3369. [PubMed: 25879388]
10. Bhatia S, Hirsch K, Bukkapatnam S, Baig NA, Oweida A, Griego A, et al. Combined EphB2 receptor knockdown with radiation decreases cell viability and invasion in medulloblastoma. Cancer Cell Int 2017;17:41 doi 10.1186/s12935-017-0409-7. [PubMed: 28360821]
11. Willson CA, Foster RD, Onifer SM, Whittemore SR, Miranda JD. EphB3 receptor and ligand expression in the adult rat brain. J Mol Histol 2006;37(8–9):369–80 doi 10.1007/s10735-006-9067-0. [PubMed: 17103029]
12. Guan XH, Lu XF, Zhang HX, Wu JR, Yuan Y, Bao Q, et al. Phosphatidylinositol 3-kinase mediates pain behaviors induced by activation of peripheral ephrinBs/EphBs signaling in mice. Pharmacol Biochem Behav 2010;95(3):315–24 doi 10.1016/j.pbb.2010.02.007. [PubMed: 20170671]
13. Yu LN, Zhou XL, Yu J, Huang H, Jiang LS, Zhang FJ, et al. PI3K contributed to modulation of spinal nociceptive information related to ephrinBs/EphBs. PLoS One 2012;7(8):e40930 doi 10.1371/journal.pone.0040930. [PubMed: 22879882]
14. Burger MT, Pecchi S, Wagman A, Ni ZJ, Knapp M, Hendrickson T, et al. Identification of NVP-BKM120 as a Potent, Selective, Orally Bioavailable Class I PI3 Kinase Inhibitor for Treating Cancer. ACS Med Chem Lett 2011;2(10):774–9 doi 10.1021/ml200156t. [PubMed: 24900266]
15. Oweida A LS, Calame D, Korpela S, Bhatia S, Sharma J, Graham C, Binder D, Serkova N, Raben D, Heasley L, Clambey ET, Nemenoff R, Karam SD. Ionizing radiation sensitizes tumors to PD-L1 immune checkpoint blockade in orthotopic murine head and neck squamous cell carcinoma. OncoImmunology 2017(In press).

16. Li S, Qin X, Chai S, Qu C, Wang X, Zhang H. Modulation of E-cadherin expression promotes migration ability of esophageal cancer cells. Sci Rep 2016;6:21713 doi 10.1038/srep21713. [PubMed: 26898709]
17. Mendez MG, Kojima S, Goldman RD. Vimentin induces changes in cell shape, motility, and adhesion during the epithelial to mesenchymal transition. FASEB J 2010;24(6):1838–51 doi 10.1096/fj.09-151639. [PubMed: 20097873]
18. Liu CY, Lin HH, Tang MJ, Wang YK. Vimentin contributes to epithelial-mesenchymal transition cancer cell mechanics by mediating cytoskeletal organization and focal adhesion maturation. Oncotarget 2015;6(18):15966–83 doi 10.18632/oncotarget.3862. [PubMed: 25965826]
19. Pecina-Slaus N Tumor suppressor gene E-cadherin and its role in normal and malignant cells. Cancer Cell Int 2003;3(1):17 doi 10.1186/1475-2867-3-17. [PubMed: 14613514]
20. Wang Y, Nakayama M, Pitulescu ME, Schmidt TS, Bochenek ML, Sakakibara A, et al. Ephrin-B2 controls VEGF-induced angiogenesis and lymphangiogenesis. Nature 2010;465(7297):483–6 doi 10.1038/nature09002. [PubMed: 20445537]
21. Sawamiphak S, Seidel S, Essmann CL, Wilkinson GA, Pitulescu ME, Acker T, et al. Ephrin-B2 regulates VEGFR2 function in developmental and tumour angiogenesis. Nature 2010;465(7297): 487–91 doi 10.1038/nature08995. [PubMed: 20445540]
22. Oweida A, Bhatia S, Hirsch K, Calame D, Griego A, Keysar S, et al. Ephrin-B2 overexpression predicts for poor prognosis and response to therapy in solid tumors. Mol Carcinog 2016 doi 10.1002/mc.22574.
23. Pasquale EB. Eph-ephrin bidirectional signaling in physiology and disease. Cell 2008;133(1):38–52 doi 10.1016/j.cell.2008.03.011. [PubMed: 18394988]
24. Pasquale EB. Eph receptor signalling casts a wide net on cell behaviour. Nat Rev Mol Cell Biol 2005;6(6):462–75 doi 10.1038/nrm1662. [PubMed: 15928710]
25. Mosch B, Reissenweber B, Neuber C, Pietzsch J. Eph receptors and ephrin ligands: important players in angiogenesis and tumor angiogenesis. J Oncol 2010;2010:135285 doi 10.1155/2010/135285. [PubMed: 20224755]
26. Cayuso J, Dzementsei A, Fischer JC, Karemore G, Caviglia S, Bartholdson J, et al. EphrinB1/EphB3b Coordinate Bidirectional Epithelial-Mesenchymal Interactions Controlling Liver Morphogenesis and Laterality. Dev Cell 2016;39(3):316–28 doi 10.1016/j.devcel.2016.10.009. [PubMed: 27825440]
27. Lui VW, Hedberg ML, Li H, Vangara BS, Pendleton K, Zeng Y, et al. Frequent mutation of the PI3K pathway in head and neck cancer defines predictive biomarkers. Cancer Discov 2013;3(7): 761–9 doi 10.1158/2159-8290.CD-13-0103. [PubMed: 23619167]
28. Swick AD, Prabakaran PJ, Miller MC, Javaid AM, Fisher MM, Sampene E, et al. Cotargeting mTORC and EGFR Signaling as a Therapeutic Strategy in HNSCC. Mol Cancer Ther 2017;16(7): 1257–68 doi 10.1158/1535-7163.MCT-17-0115. [PubMed: 28446642]
29. Ottone C, Krusche B, Whitby A, Clements M, Quadrato G, Pitulescu ME, et al. Direct cell-cell contact with the vascular niche maintains quiescent neural stem cells. Nat Cell Biol 2014;16(11): 1045–56 doi 10.1038/ncb3045. [PubMed: 25283993]

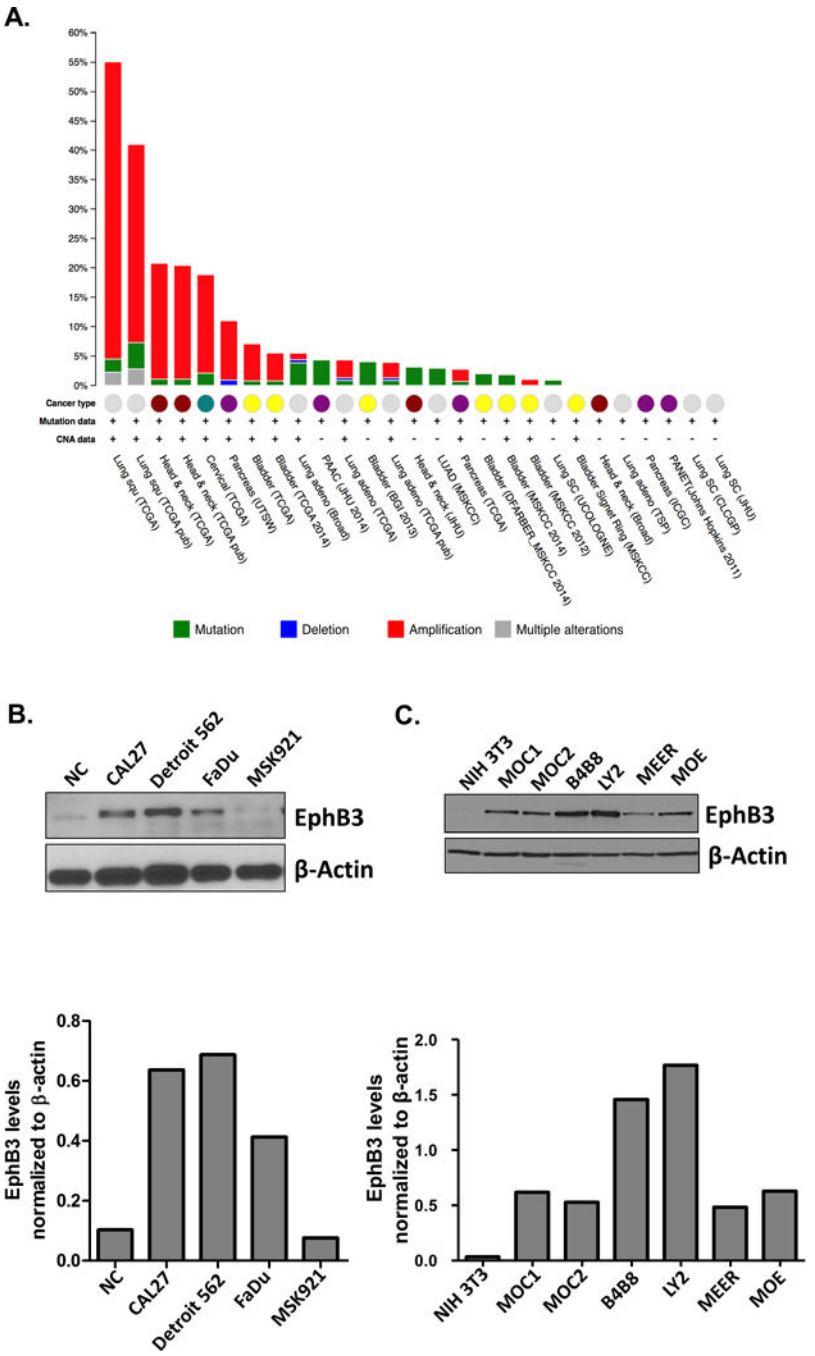


**Figure 1. EphB3 is amplified in head and neck squamous cell carcinomas.**

Query of alterations in EphB3 across all cancer types was performed using data from TCGA via cBioPortal (A). Western blot analysis reveals differential levels of EphB3 in both human (B) and mouse head and neck cancer cells (C).

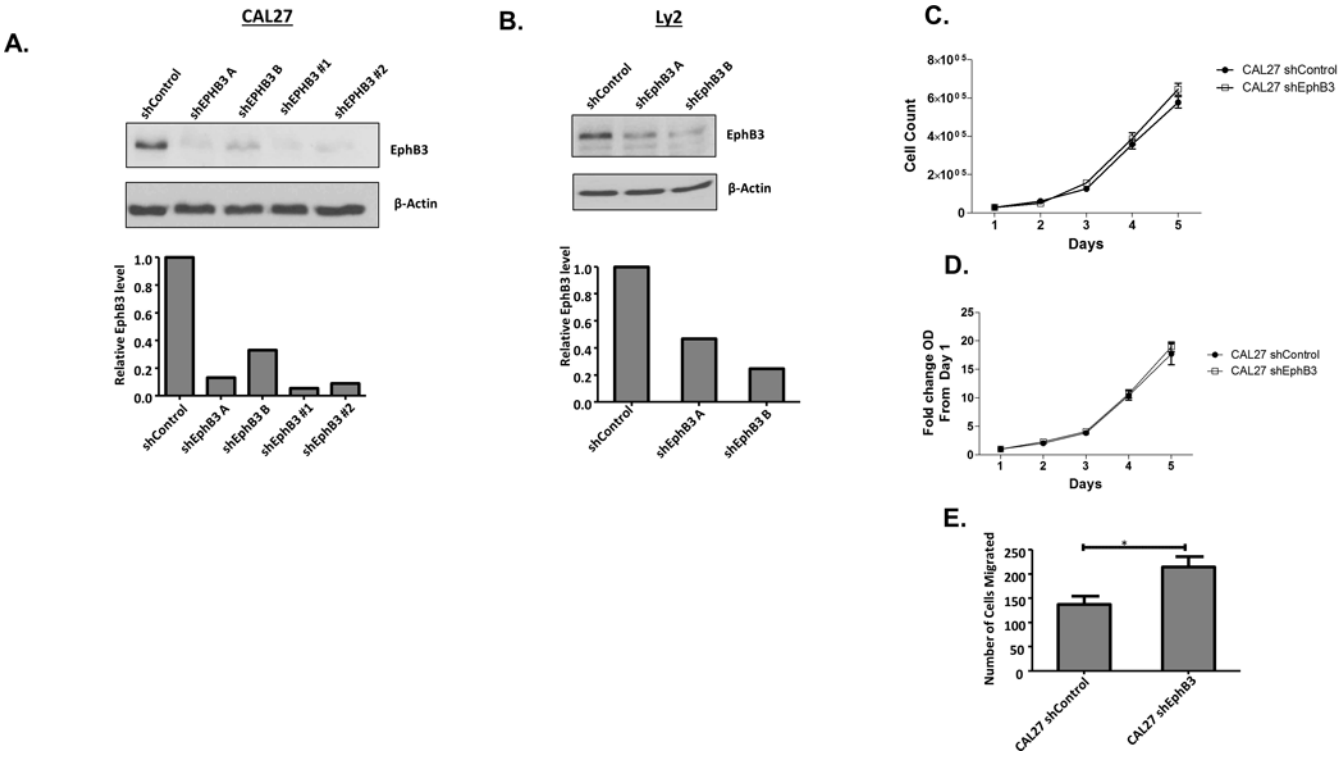


**Figure 2. EphB3 knockdown does not affect tumor cell viability but enhances cell migration in head and neck cancer cell lines.**

Knockdown of EphB3 was conducted by retrovirally transducing CAL27 (A) and Ly2 cells (B) with control or EphB3-specific shRNA. Effect of EphB3 knockdown on CAL27 cell viability was assayed at 72 h post-plating by trypan blue exclusion assay (C) and SRB assay (D). Effect of EphB3 knockdown on Cal27 cell migration was assayed by Boyden chamber (E). Cells were allowed to migrate for 48 h prior to fixing and staining. Number of cells migrated through the membrane were counted. Data are the result of 2–3 experiments performed in duplicate. Error bars represent the SEM. *$p<0.05$

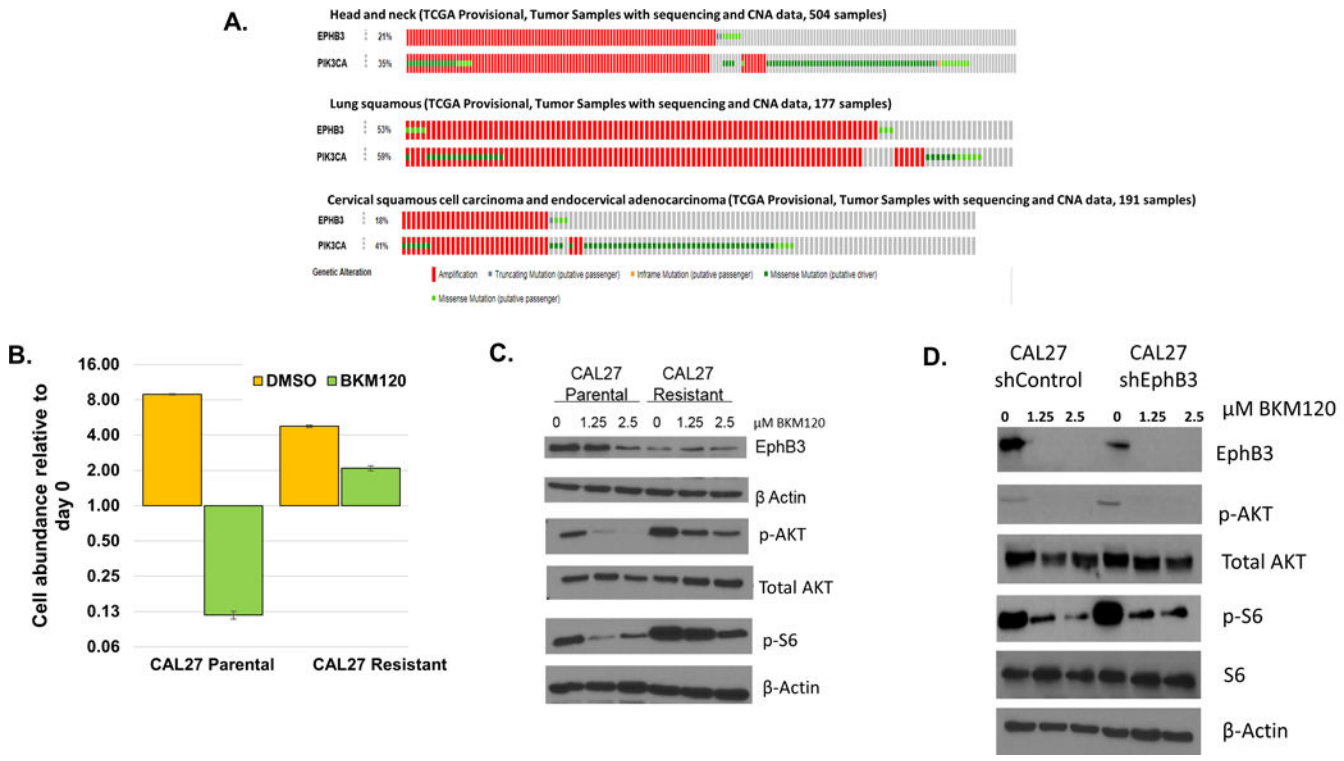


**Figure 3. EphB3 knockdown decreases response to PI3K inhibitor and alters the expression of pro-survival molecules.**

Amplification of PIK3CA genomic alterations were queried for cancers with the highest percentage of EphB3 amplification (A). (B) SRB assay performed on CAL27 parental and BKM120 resistant cell lines treated with 2 μM dose BKM120 show modified response on tumor cell growth at 72 h time-point. (C) EphB3 protein levels are analyzed in CAL27 parental and BKM120 “resistant” cell lines following exposure to the indicated concentrations of BKM120 for 24 h. Effects on p-AKT, AKT, and p-S6 (a key regulator of AKT) were also determined in both parental and BKM120 resistant cell lines. (D) Effects on p-AKT, total AKT, p-S6, and S6 are determined on Cal 27 cell line transfected with Control shRNA and EphB3 shRNA with vehicle or BKM120 treatment.

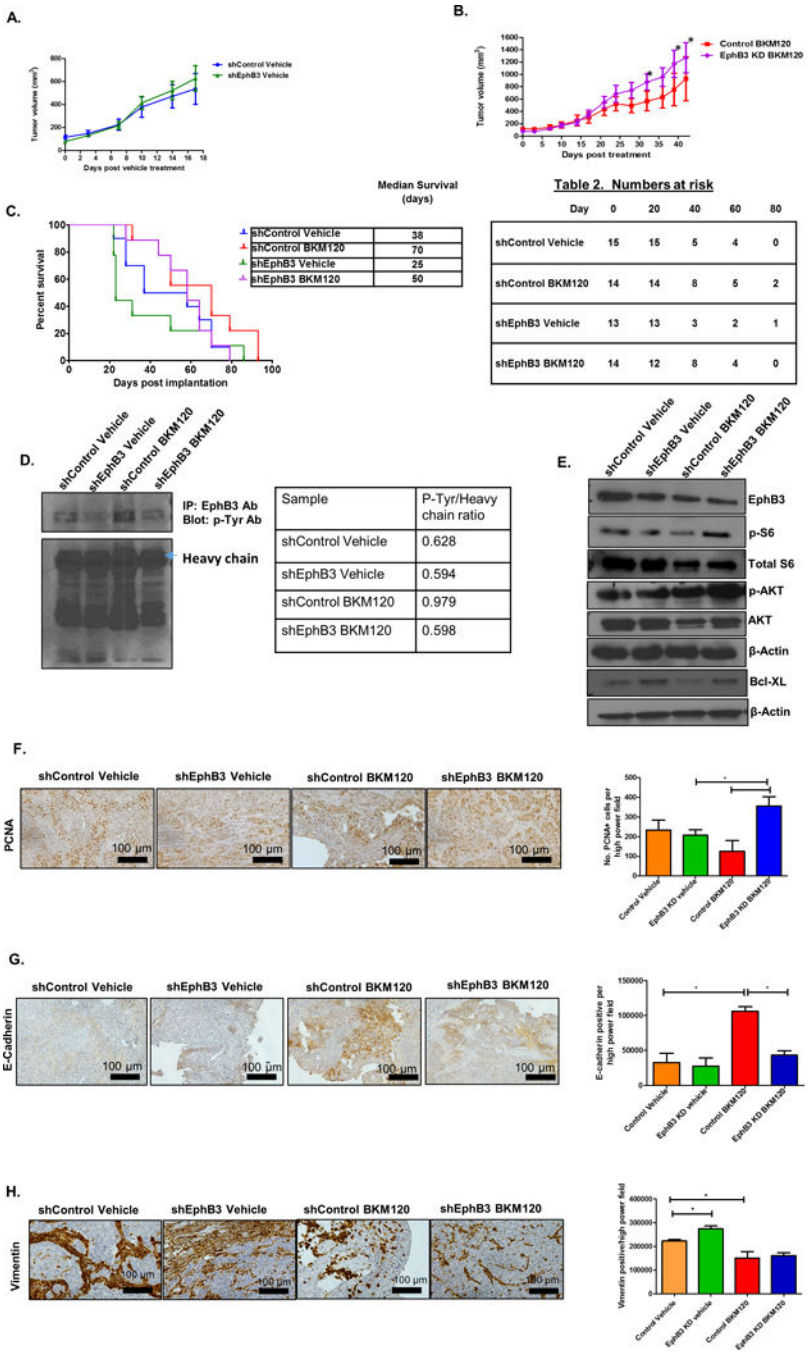


**Figure 4. Knockdown of EphB3 receptor does not affect tumor growth and decreases sensitivity to PIK3CA inhibitor, BKM120, in an orthotopic model of head and neck cancer.**

Athymic nude mice are injected with CAL27 cells, transfected with either control shRNA or EphB3 specific shRNA (EphB3 KD), in the buccal region and treated with either vehicle or BKM120 daily (30 mg/kg) for two weeks. Tumors were allowed to grow to protocol limits. Due to the aggressive tumor growth pattern, most of the mice in the EphB3 knockdown and control group subjected to vehicle treatment were sacrificed after day 20 post-vehicle treatment. Tumor growth volume curves did not show any significant difference in tumor volumes between control and EphB3 knockdown tumors that received vehicle treatment (A).

Tumor volume data show increased tumor growth in EphB3 knockdown tumors treated with BKM120 compared to the control shRNA tumors that were subjected to the same treatment. The difference in tumor growth between Control and EphB3 knockdown tumors with BKM120 treatment was significant ($p<0.05$) at day 42 post inhibitor administration. (B). Survival curve and median days of survival post tumor cell implantation shows significant difference between the tumors administered with vehicle vs. BKM120 ($p=0.0235$) (C). Immunoprecipitation analysis show alteration in the levels of p-EphB3 in the control vs. EphB3 knockdown tumors treated with vehicle or BKM120 inhibitor (D). Cal 27 tumors knocked down for EphB3 receptor show small increase in the levels of key pro-survival protein p-S6 in the presence of BKM120 compared to the cells where EphB3 is intact (E). Representative images of PCNA (F), E-cadherin (G), and Vimentin (H) are shown. Immunohistochemical staining was used to evaluate changes in control and EphB3 knockdown tumors treated with vehicle or BKM120. In the EphB3 knockdown tumors treated with BKM120, a significant enhancement in the levels of PCNA was observed. This was accompanied by a decrease in the levels of E-cadherin compared to the control tumors that received same treatment.

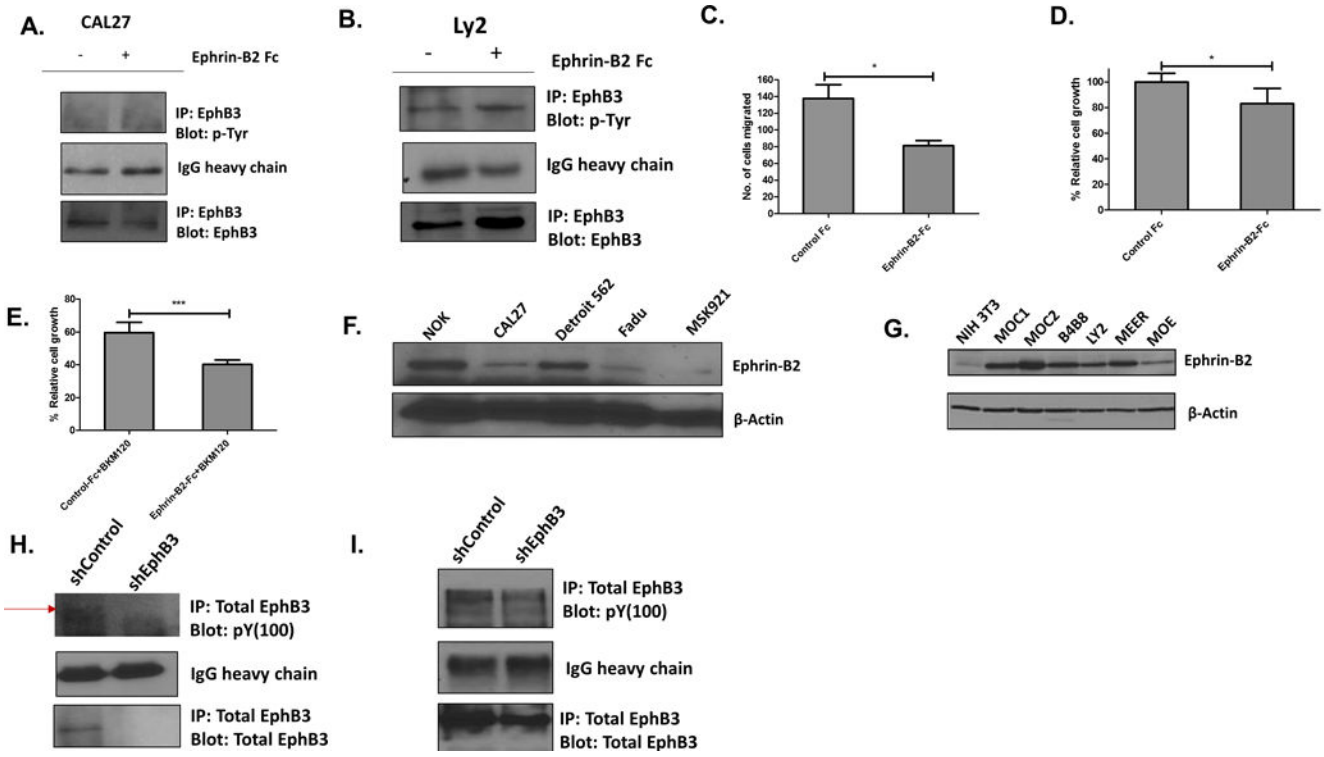


**Figure 5. Forced phosphorylation of EphB3 receptor with ephrin-B2 Fc reduces tumor cell migration and cell growth and enhances responsiveness to BKM120 *in vitro.***

Phosphorylation status of EphB3 in CAL27 (A) and Ly2 (B) cells in the absence and presence of ephrin-B2-Fc stimulation was analyzed by immunoprecipitation with total EphB3 antibody and probed for total phosphotyrosine. Tumor cell migration was analyzed in CAL27 cells stimulated with control Fc or ephrin-B2 Fc at 72 h by Boyden chamber assay and showed significant reduction in the number of migrated cells in the presence of ephrin-B2 Fc (C). Changes in cell growth was determined by an MTT assay in the presence of Control Fc or Ephrin-B2-Fc stimulation of Cal27 cells. Data showed a significant decrease in cell growth in ephrin-B2-stimulated group at 128 h post-stimulation (D). Treatment of CAL27 cells with BKM120 (2 uM) also showed a significant decline in cell growth following ephrin-B2 stimulation (128 h post-stimulation) compared to the control counterparts (E). Western blot analysis show variable levels of ephrin-B2 ligand in human HNSCC (F) and mouse HNSCC cell lines (G). Mouse cell line samples analyzing for EphB3 (Figure 1C) and ephrinB2 levels were run at the same time and share same β-actin control. Immunoprecipitation analysis in CAL27 cells (H) and Ly2 cells (I) show reduced p-EphB3 levels in the knockdown clones compared to the control counterparts.

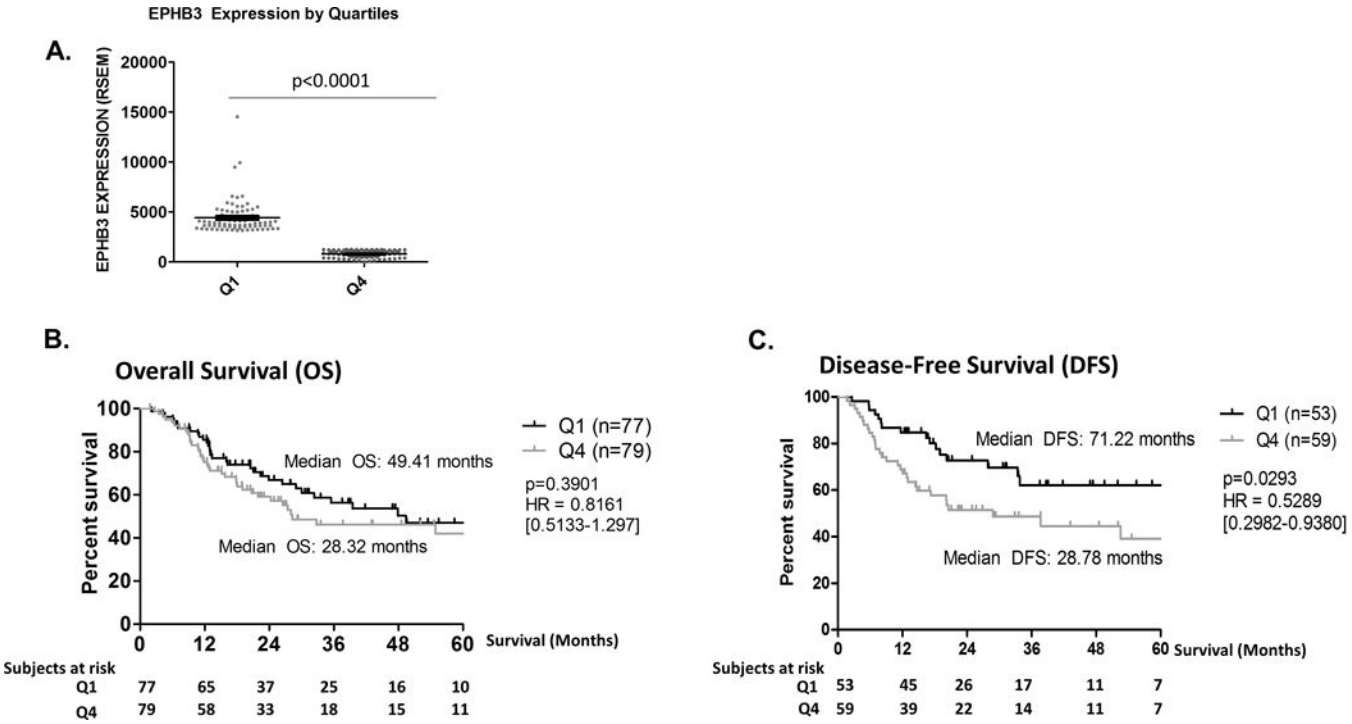


**Figure 6. Elevated levels of EphB3 correlates with better survival in head and neck cancer patients.**

Analysis was performed on HNSCC RNAseq dataset downloaded from The Cancer Genome Atlas (TCGA). Patients (n=314) with oral cavity tumors were sorted by EPHB3 gene expression and divided into quartiles (A) RSEM indicates RNA-Seq by Expectation Maximization. Further analysis show that elevated level of EphB3 improves overall survival (B) and disease-free survival (C) of head and neck squamous cell carcinoma patients.

**Table 1.**

Percentage of patients with co-amplification of EPHB3 and PIK3CA, a subunit of PI3 Kinase in human cancers

| Cancer type | Percent of all patients with co-amplified gene alteration | p-Value | Log Odds ratio |
|---|---|---|---|
| HNSCC | 20.40 | <0.001 | <3 |
| Lung SCC | 43.06 | <0.001 | <3 |
| Cervical SCC and Adenocarcinoma | 18.77 | <0.001 | <3 |

Abbreviations: HNSCC, head and neck squamous cell carcinoma; SCC, squamous cell carcinoma

**Table 2.**

Densitometric analysis of CAL27 parental and resistant cells exposed to vehicle or BKM120

| CAL27 | BKM120 (μM) | EphB3/β-actin | p-AKT/AKT | AKT/β-actin | p-S6/β-actin |
|---|---|---|---|---|---|
| Parental | 0 | 1.31 | 1.13 | 0.51 | 0.98 |
| Parental | 1.25 | 1.21 | 0.87 | 0.51 | 0.75 |
| Parental | 2.5 | 0.96 | 0.91 | 0.44 | 0.77 |
| Resistant | 0 | 0.86 | 1.42 | 0.48 | 1.15 |
| Resistant | 1.25 | 0.94 | 1.10 | 0.51 | 1.09 |
| Resistant | 2.5 | 1.03 | 0.98 | 0.54 | 0.92 |

**Table 3.**

Densitometric analysis of CAL27 shControl and shEphB3 cells exposed to vehicle or BKM120

| CAL27 | BKM120 (μM) | p-AKT/AKT | AKT/β-actin | p-S6/β-actin | p-S6/β-actin |
|---|---|---|---|---|---|
| shControl | 0 | 0.23 | 1.55 | 1.54 | 1.44 |
| shControl | 1.25 | 0.27 | 1.31 | 0.99 | 1.67 |
| shControl | 2.5 | 0.24 | 1.48 | 0.94 | 1.57 |
| shEphB3 | 0 | 0.26 | 1.54 | 1.69 | 1.57 |
| shEphB3 | 1.25 | 0.23 | 1.38 | 1.01 | 1.48 |
| shEphB3 | 2.5 | 0.24 | 1.33 | 0.99 | 1.56 |